Implications of the theory of turbulent mixing for wave propagation in media with fluctuating coefficient of refraction

Jaan Kalda[*] and Mihkel Kree

Institute of Cybernetics, Tallinn University of Technology, Akadeemia tee 21, 12818 Tallinn, Estonia

Abstract. Based on ray tracing approach, light propagation in inhomogeneous media with fluctuating coefficient of refraction $n = n(\mathbf{r})$ can be interpreted as a chaotic mixing of the wavefront in the 6-dimensional phase space where the spatial coordinates are complemented by the respective wave vector components. According to ray tracing, the evolution of wave vectors follows Hamiltonian dynamics and hence, according to the Liouville's theorem, the mixing of the wave front takes place in an incompressible flow field. We use this approach to show that the brightest light speckles in inhomogeneous media follow a power law intensity distribution, and to derive the relevant scaling exponents.

Key words: light propagation in inhomogeneous media, chaotic mixing.

1. INTRODUCTION

Propagation of waves (and of electromagnetic waves, in particular) in fluctuating media has been studied extensively for a long time, c.f. reviews [1–3]. One particularly important application of the results of such studies is the propagation of light in turbulent atmosphere: the distortion of wavefronts hinders Earth-based astronomical observations and is being dealt with adaptive optics. Another important application is the sound propagation in water of varying temperature and salinity.

Perhaps the most well known feature of the wave propagation in inhomogeneous media is the appearance of caustics, which emerge already in homogeneous media (for instance, water) if the interface (e.g. the water surface) is uneven. Speckle formation is further enhanced by wave propagation through inhomogeneities. For many practical applications, the fluctuations of the refractive index are relatively small: this applies both to the atmospheric turbulence, and to the water reservoirs of fluctuating temperature and salinity. Strong fluctuations of the refractive index are possible for sound propagation in heterogeneous media, for plasma waves in ultrasonic plasma turbulence, and light propagation in multiphase media.

In many practical cases, the distortion of wavefronts remains relatively weak. The strength of distortions can be characterized by the number of how many times the wavefront is folded. More specifically, we take a line parallel to the initial direction of the wave, and count, how many times (N) the wavefront intersects this line. This number is related (but not identical) to another number, characterizing the distortions – the number of speckles (bright spots) when attempt is made to focus the beam, e.g. through telescopes. Indeed, while $N > 1$ means necessarily that there are many speckles at the focal plane, the opposite is not true: at the focal plane, many speckles can appear already when the wavefront is not folded ($N = 1$); the number of such speckles depends on the aperture of the focusing device. In the case of light propagation through atmospheric turbulence, the degree of distortions depends on the travelled distance, strength of turbulence, and the scale at which the wavefront is resolved.

In what follows we address the strong wavefront distortion limit $N \gg 1$: we reduce the problem of speckle intensity distribution to the problem of turbulent mixing by incompressible velocity field in six-dimensional phase space. This approach is based on representing the evolution of wave vectors as a Hamiltonian dynamics, and applying the Liouville theorem. While the Liouville

* Corresponding author, kalda@ioc.ee

theorem has been applied in this context earlier, see [4], the theoretical results of turbulent mixing have not been invoked to address the problem of speckle intensity distribution.

Reducing the problem of wave propagation in inhomogeneous media to the problem of turbulent mixing is highly useful: trubulent diffusion has been studied for a very long time, and there is a long list of theoretical achievements [5–15].

2. WAVE PROPAGATION IN INHOMOGENEOUS MEDIA AS A CHAOTIC MIXING OF WAVEFRONT IN PHASE SPACE

We consider situation when a regular wavefront (which is assumed for the sake of simplicity to be flat) enters an inhomogeneous medium. Then, we can study the dynamics of a point on the wavefront, described by the coordinate of the given point r and the wave vector k. Both r and k are functions of time t, and their evolution equation can be written in Hamiltonian form as

$$
\begin{aligned}
\partial_t k &= -\partial_r |k|/n(r), \\
\partial_t r &= \partial_k |k|/n(r),
\end{aligned}
\tag{1}
$$

where $n = n(r)$ is the fluctuating coefficient of refraction. By writing these equations we assume that $n = n(r)$ is a smooth function of the coordinates r, and that the characteristic scale of variations is larger than the wavelength.

When a flat wave enters the medium along the z-axis so that at $t = 0$ the initial wave vector is everywhere equal to $k(0) = k_0 e_z$, the entire wavefront corresponds to a 2-dimensional surface in the 6-dimensional phase space, given by the conditions

$$
r \cdot e_z = 0, \quad k = k_0 e_z;
\tag{2}
$$

here, e_z stands for a unit vector along the z-axis. This 2-dimensional surface starts evolving according to the equations (1); we can consider it as a tracer in the flow field given by Eqs (1). According to the Liouville theorem, this flow field is incompressible. The wave energy is also transferred through the space according to the Eqs (1). Hence, the wave energy becomes as many times diluted as many times the wavefront is stretched. Thus, the problem of finding energy density distribution in space is reduced to the problem of finding the stretching statistics of a material surface (the wavefront) in incompressible flow field.

When applying the above described mapping, few circumstances need to be kept in mind. First, our aim is to find statistical features of energy density distribution in the coordinate r space, so we need to project the wave energy field from the phase space to the real coordinate space. As a result of such a projection, different wave-front fragments may overlap; then, the respective energy densities need to be added up. This means that there is no strict one-to-one correspondence between the speckle distribution, and the stretching factor statistics. However, in the case of the brightest speckles (the least stretched areas), the matching is nearly perfect because if a bright speckle is overlapped by dim speckles, the bright speckle dominates heavily: the log-normal distribution assumes that the speckle brightness varies typically by several octaves. Second, we have ignored the effect of diffraction and interference. For light sources of moderate coherence length, interference can be easily neglected: different speckles add up in random phases. Diffraction can be neglected as long as the speckle size becomes of the order of the wavelength; below that, diffraction results in an effective smudging of speckles over a wavelength. Third, we have ignored the formation of caustics, which are known to appear at the early stages of wave propagation in inhomogeneous media. At the later stages, however, the strong intensity fluctuations due to the log-normal light energy distribution dominates over the intensity fluctuations due to the caustics.

3. SIZE-DISTRIBUTION OF TRACER PATCHES IN INCOMPRESSIBLE CHAOTIC FLOWS

The stretching statistics of material elements (surfaces, lines, etc.) in chaotic velocity fields are quite well studied and known, because this information is used to derive the behaviour of the tracer fields in turbulence at the limit of large Peclet' numbers, $\mathrm{Pe} = av/\kappa$, where a and v are the characteristic scale and characteristic speed of the flow, respectively, and κ is the molecular diffusivity [5]. It is well known that in the case of smooth velocity fields (i.e. if there is no turbulent cascade, or we look at the flow with good enough resolution so that the smallest vortices are resolved and the streamlines look locally smooth), the stretching factor s distribution follows a log-normal distribution,

$$
dP = (4t\pi)^{-1/2} e^{-(\ln s - ut)^2/4t} d\ln s,
\tag{3}
$$

where t is a properly renormalized dimensionless time, and u is the parameter describing the flow [5]. The time renormalization is done so that the process $\ln s = f(t)$ would correspond to a random walk of unit diffusivity. This distribution explains, for instance, the multifractality of tracer dissipation fields [16], and gives rise to various power laws of the tracer fields [17,18]. Apart from the evolution time t, this distribution has only one parameter, u, which, in the case of incompressible ideal Kraichnan flows (delta-correlated in time), equals to the dimensionality of the flow. Recently it has been shown that in the case of real flows, this parameter can take slightly larger values [19]. In the case of non-smooth velocity fields, Eq. (3) is no longer applicable, and instead, one is forced to work with the probability density functions for pair dispersion of material particles [20]. Here, however, we shall be assuming that the fluctuations of refraction index are smooth, which means that the streamlines are smooth, as well.

Note that Eq. (3) describes not only the distribution of local stretching factors, but also the distribution of the distance between two material particles which were initially seeded at a fixed small distance from each other, as long as the distance remains smaller than the viscous dissipation scale. Meanwhile, the process described by it is qualitatively different from ordinary diffusion as in that case, the pair distance distribution will evolve towards a Gaussian profile in *linear length scale* (and not in logarithmic scale).

Based on Eq. (3), one can easily derive a power law size-distribution for the tracer patches. Indeed, if we have initially a small rectangular patch of tracer, smaller than the characteristic scale of the flow so that the rectangle will evolve into a parallelepiped (the result can be generalized to other shapes, as well). Then, due to the volume conservation, the thickness of the patch is inversely proportional to the surface area of its edge in 3-dimensional geometry, and to the side length in the case of 2-dimensional geometry. In what follows we shall be using 2-dimensional geometry, but the results can be easily generalized to the 3-dimensional geometry.

Now, if we had initially many tracer patches (or one longer patch), the number of patches of thickness exceeding a fixed threshold value δ_0 scales as the probability for the stretching coefficient being smaller than the corresponding threshold value $s_0 = b/\delta_0$, where b is the initial thickness of the tracer patch:

$$N \propto e^{-(\ln \delta_0 + ut)^2/4t} \propto \delta_0^{-\frac{u}{2} - \frac{\ln \delta_0}{4t}}. \tag{4}$$

This scaling law can be rewritten in terms of the patch thickness as

$$N \propto \delta_0^{-\gamma}, \ \ \gamma = \frac{u}{2} + \frac{\ln \delta_0}{2t}. \tag{5}$$

It should be noted that what we have obtained is not a perfect scaling law: the exponent γ is a function of the patch diameter. However, the dependence is slow, logarithmic, and can be often neglected.

We have checked this scaling law using the photographs of the dye patterns recorded at the CORIOLIS tank in Grenoble in 1996, during the experiments supported by PECO/COPERNICUS project ERBCIPD940092/ERBCHGECT920015 and supervised by Prof. Tarmo Soomere. A fluorescent dye has been injected into the quasi-two-dimensional high-vorticity flow in the tank. The dye has been illuminated by a rotating laser and periodically recorded to a high sensitivity film (ISO 1600). The analysis is based on such images which correspond to the time interval between the injection of the dye and taking the snapshot equal to approximately 20 eddy turnover times; one such photograph is shown in Fig. 1.

Fig. 1. A photo of the dye patterns recorded at the CORIOLIS tank in Grenoble in 1996 and used to obtain the graph in Fig. 2. A fluorescent dye has been injected into the quasi-two-dimensional high-vorticity flow in the tank; the dye was illuminated by a rotating laser and the patterns were periodically recorded by taking photos.
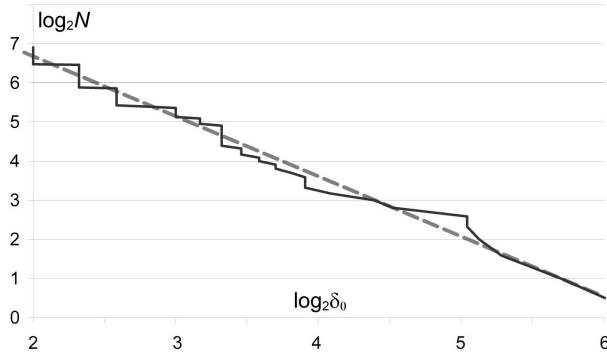
Fig. 2. The number of patches with thickness exceeding a threshold value δ_0 (measured in the number of pixels on digitized photos); the data are represented in a log-log plot, so that a straight line would correspond to a power law predicted by Eq. (5); here, $\gamma \approx 1.5$.

For each such snapshot, equispaced intersection lines had been drawn, and along each intersection line, the number of patches of thickness exceeding the threshold value δ_0 has been counted. The results are shown in Fig. 2 using log-log scale. Unfortunately, the exact value for the parameter u, describing the underlying velocity fields, is not available. However, an approximate value can be deduced from general considerations: while for 2-dimensional Kraichnan flows $u = 2$, in the case of moderate Kubo numbers, values $u \in [2.2, 2.5]$ can be expected [19]. While the data are provided here without a proper error analysis, a nearly linear trend implies a qualitative agreement with the theory, and the degree of fluctuations is indicative of the statistical uncertainties. In order to obtain lower uncertainties so that the prediction of Eq. (5) about scale-dependence of the scaling exponent could be verified, higher resolution experimental data are required.

4. MIXING IN PHASE SPACE

According to what has been said above, the power law exponent in the scaling law (5) is defined mainly by the parameter u. While in the case of statistically isotropic homogeneous delta-correlated-in-time flows, u equals to the dimensionality of the space (this would correspond to $u = 2$ for the data of Fig. 1), c.f. [5], for real time-correlated flows it has somewhat larger values, typically increased by few decimal digits [19]. The phase space dimensionality is six, but the flow is constrained to a five-dimensional subspace defined by the energy conservation law: as long as the refraction index fluctuations can be considered to be constant in time, the wave frequency remains constant during the wave propagation. This would infer $u \approx 5$; however, the flow in our phase is by no means isotropic.

In order to understand what is going on, let us consider the simplest case when the dimensionality of

the phase space is effectively reduced down to two, and assume that there are only small refraction index variations, and no dependence on the third spatial coordinate z, so that $n = n(x, y)$ with $|n(x, y) - 1| \ll 1$. Let the incident light beam be initially parallel to the y-axis, so that initially, $k_x \equiv 0$. Then we can ignore both the variations of the modulus of $\boldsymbol{k}$ (due to the frequency invariance), and the variations of k_y, assuming that the observation time is not too long, so that the angle between the wave vector and the x-axis remains small. Then, the elapsed time can be also determined from the current value of the y-coordinate of the wavefront. We can use such units that the speed of light equals to unity, in which case $y = t$, and the process can be approximated by the following equations:

$$\dot{k}_x = -\partial_x \left[\frac{k_x^2}{2} - n(x, t) \right],$$

$$\dot{x} = \partial_{k_x} \left[\frac{k_x^2}{2} - n(x, t) \right]; \tag{6}$$

here, dot denotes the time derivative. This describes a mixing in 2-dimensional geometry by a perturbed shear flow, sketched in Fig. 3. Note that this process is very similar to the velocity distribution function mixing in the case of nonlinear Landau damping, except that we have a random time-dependant potential.

While this velocity field is by no means statistically isotropic, one can notice the following. During the process, every segment of wavefront is being rotated and over a longer time span, all the possible orientations are taken. Hence, one can expect that the wavefront "feels" essentially an isotropic stretching, so that still $u \approx 2$. This conjecture will be shown to be valid in the next Section using simulation data.

In a similar way we can analyse the wavefront mixing under the assumption of weak refraction index variations in the full three-dimensional geometry. Then,
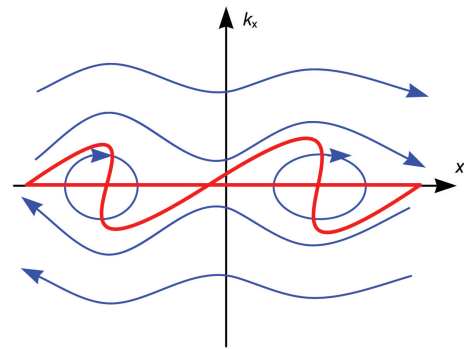

Fig. 3. A sketch of wavefront (depicted with bold lines for two different moments of time) which is being mixed by a perturbed shear flow as described by Eq. (6). Solid lines with arrows depict the streamlines at a certain moment of time.

if the incident beam is directed along the z-axis, the evolution equations are written as

$$\dot{k}_x = -\partial_x \left[\frac{k_x^2 + k_y^2}{2} - n(x, y, t) \right],$$

$$\dot{x} = \partial_{k_x} \left[\frac{k_x^2 + k_y^2}{2} - n(x, y, t) \right],$$

$$\dot{k}_x = -\partial_y \left[\frac{k_x^2 + k_y^2}{2} - n(x, y, t) \right], \quad (7)$$

$$\dot{x} = \partial_{k_y} \left[\frac{k_x^2 + k_y^2}{2} - n(x, y, t) \right].$$

This system of equations tells us that while the wavefront dynamics in the two-dimensional subspaces of $x - k_x$ and $y - k_y$ is very similar to what was observed in the case of Eqs (6), there is no wavefront rotations from one subspace to the other. Hence, we can expect independent wavefront stretching in two subspaces, both described by $u = 2$. Based on this, we can also analyse the dynamics of the material line length in the full four-dimensional space. Indeed, according to the Pythagorean theorem, the squared length of a small piece of material line is given by the sum of the squares of the corresponding lengths in the 2-dimensional subspaces: $L^2 = l_1^2 + l_2^2$, where both l_1 and l_2 follow log-normal distribution (Eq. (3)) with $u = 2$. Asymptotically, typical differences between the lengths l_1 and l_2 are huge, hence the probability of having the same order of values for both l_1 and l_2 is negligible. This means that the smaller term can be neglected and we can write

$$L = \max(l_1, l_2). \quad (8)$$

It can be shown that asymptotically, L follows also a log-normal distribution; the respective parameter value u can be obtained as the ratio of the mathematical expectation and variance of $\ln \max(l_1, l_2)$. The corresponding integrals can be taken analytically, yielding $u = \frac{2\pi}{\pi - 1} \approx 2.9$.

5. SIMULATION RESULTS

Simulations have been based on Eqs (6) and (7) using sinusoidal refraction index variations:

$$n(x) = 1 + A \sin(2\pi/\lambda x + \varphi), \quad (9)$$

for 2-dimensional geometry, and

$$n(x, y) = 1 + A \sin[2\pi/\lambda (x \cos \beta + y \sin \beta) + \varphi] \quad (10)$$

for the 4-dimensional one. Here, the amplitude was fixed to $A = 0.05$, and the phase φ and angle β are random variables with constant probability distribution which retain constant values during one correlation time, and take new random values after that. The modulation wavelength was kept equal to $\lambda = 50$. A typical shape of the
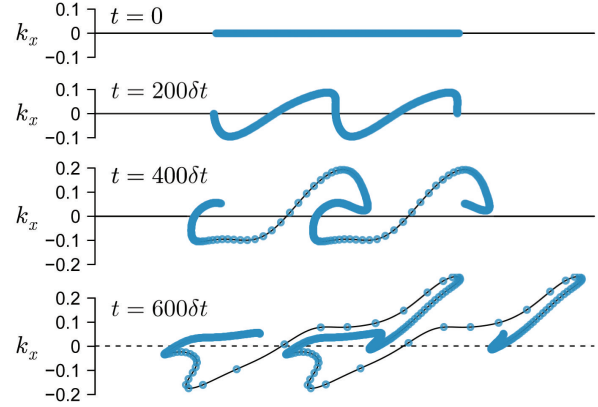

Fig. 4. Typical shapes of the wavefront emerging from numerical simulations according to Eqs (6) and (9) for different evolution times; δt stands for the correlation time.

wavefront in the case of 2-dimensional geometry is depicted in Fig. 4.

The simulation results for 2-dimensional geometry yielded $u \approx 1.84 \pm 0.04$; this is somewhat less than the theoretical result $u = 2$ for Kraichnan flows; finite correlation times make the parameter larger and hence, cannot explain the mismatch. Another option would be to ascribe this mismatch to finite-size scaling effects caused by finite simulation time. However, our simulations show that the asymptotic behaviour has been reached: even if the calculation time is increased by a factor of two, the results remain still the same. Therefore, we can conclude that due to strong anisotropy of the velocity field, the isotropic two-dimensional mixing regime with $u = 2$ is not achieved: the parameters of the log-normal distribution of the material line stretching coefficients behave as if the dimensionality of the flow were somewhat less than two. The same applies to the simulations for 4-dimensional geometry: the numerically obtained value $u \approx 3.3 \pm 0.1$ is slightly more than the expected value of $u = \frac{2\pi}{\pi - 1}$, but less than $u = 4$, which corresponds to the isotropic four-dimensional geometry. Overall, the simulations show that while the velocity field anisotropy incurs small changes in the parameters of the log-normal distribution, the departure from the case of isotropic turbulence remains small.

6. CONCLUSIONS

We have shown above that the problem of finding speckle intensity distribution for wave propagation in inhomogeneous media can be mapped to the problem of mixing in incompressible flows. This means that the intensity distribution is log-normal, and is described by two parameters: the parameter u in Eq. (3) which is mostly defined by the dimensionality of the space, and the mixing time t. We have also shown that the size distribution of the largest tracer patches in turbulent flows, and hence, the intensity distribution of

the brightest speckles is approximated reasonably well by a power law.

The simulations confirm log-normal ditribution of the wavefront stretching in phase space for light propagation in media of weakly fluctuating refraction index, and show that the wavefront mixing takes place almost independently in two 2-dimensional subspaces of the 4-dimensional phase space. Currently we have no simulation data for wavefront mixing in the case of strong refraction index fluctuations. While we can hypothesize that in the case of strong refraction index fluctuations, the wavefront is mixed effectively isotropically in a 5-dimensional subspace of the 6-dimensional phase space (the subspace being defined by the wave frequency conservation law), which would lead to $u \approx 5$, further numerical simulations are needed for a definite conclusion.

ACKNOWLEDGEMENTS

REFERENCES

1. Wheelon, A. D. *Electromagnetic Scintillation: Volume 1, Geometrical Optics*. Cambridge University Press, Cambridge, UK, 2001.

2. Korotkova, O. *Random Light Beams: Theory and Applications*. Taylor and Francis, Hoboken, NJ, 2013.

3. Klyatskin, V. I. Electromagnetic wave propagation in a randomly inhomogeneous medium as a problem in mathematical statistical physics. *Physics–Uspekhi*, 2004, **47**(2), 169–186.

4. Bal, G., Komorowski, T., and Ryzhik, L. Kinetic limits for waves in a random medium. *Kinetic and Related Models*, 2010, **3**(4), 529–644.

5. Falkovich, G., Gawędzki, K., and Vergassola, M. Particles and fields in fluid turbulence. *Rev. Mod. Phys.*, 2001, **73**(4), 913–975.

6. Richardson, L. F. Atmospheric diffusion shown on a distance-neighbour graph. *P. Roy. Soc. Lond. A Mat.*, 1926, **110**, 709–737.

7. Batchelor, G. K. Small-scale variation of convected quantities like temperature in turbulent fluid. Part 1. General discussion and the case of small conductivity. *J. Fluid Mech.*, 1959, **5**, 113–133.

8. Aref, H. Stirring by chaotic advection. *J. Fluid Mech.*, 1984, **143**, 1–21.

9. Ottino, J. M. Mixing, chaotic advection, and turbulence. *Annu. Rev. Fluid Mech.*, 1990, **22**(1), 207–254.

10. Sreenivasan, K. R. and Antonia, R. A. The phenomenology of small-scale turbulence. *Annu. Rev. Fluid Mech.*, 1997, **29**(1), 435–472.

11. Warhaft, Z. Passive scalars in turbulent flows. *Annu. Rev. Fluid Mech.*, 2000, **32**(1), 203–240.

12. Dimotakis, P. E. Turbulent mixing. *Annu. Rev. Fluid Mech.*, 2005, **37**(1), 329–356.

13. Shraiman, B. I. and Siggia, E. D. Scalar turbulence. *Nature*, 2000, **405**, 639–646.

14. Toschi, F. and Bodenschatz, E. Lagrangian properties of particles in turbulence. *Annu. Rev. Fluid Mech.*, 2009, **41**(1), 375–404.

15. Grabowski, W. W. and Wang, L.-P. Growth of cloud droplets in a turbulent environment. *Annu. Rev. Fluid Mech.*, 2013, **45**(1), 293–324.

16. Kalda, J. Simple model of intermittent passive scalar turbulence. *Phys. Rev. Lett.*, 2000, **84**(3), 471–474.

17. Kalda, J. On the multifractal properties of passively convected scalar fields. In *Paradigms of Complexity. Fractals* (Novak, M., ed.). World Scientific, Singapore, 2000, 193–201.

18. Kalda, J. k-spectrum of decaying, aging and growing passive scalars in Lagrangian chaotic fluid flows. *J. Phys. Conf. Ser.*, 2011, **318**(5), 052045.

19. Ainsaar, S. and Kalda, J. On the effect of finite-time correlations on the turbulent mixing in smooth chaotic compressible velocity fields. *Proc. Estonian Acad. Sci.*, 2015, **64**, 1–7.

20. Kalda, J. Sticky particles in compressible flows: aggregation and Richardson's law. *Phys. Rev. Lett.*, 2007, **98**(6), 064501.

Turbulentse segunemise teooria rakendusi lainelevile muutuva murdumisnäitajaga keskkonnas

Jaan Kalda ja Mihkel Kree

Lainelevi muutuva murdumisnäitajaga $n = n(\boldsymbol{r})$ keskkonnas on geomeetrilise optika lähenduses kirjeldatav Hamiltoni dünaamikana lainevektori ja lainefrondi jaoks. Tulenevalt Liouville'i teoreemist tähendab see, et lainefront areneb faasiruumis kui kuuedimensioonilise kokkusurumatu kiirusvälja edasikantav passiivne skaalar. Seda asjaolu kasutades näitame, et aja jooksul jaguneb laineenergia väikestesse suure energiaga piirkondadesse, mida nimetame valgustäppideks. Nende jaotumine energia järgi allub astmeseadusele; vastava astmenäitaja jaoks tuletame analüütilise avaldise. Astmenäitaja avaldises sisalduva, efektiivset kiirusvälja dimensioonilisust kirjeldava parameetri leiame numbriliselt. Eksperimentaalandmetele tuginedes näitame, et vastav astmeseadus kehtib ka passiivse skaalari segunemisel kahedimensioonilises kaootilises kiirusväljas.